



## Adsorption of Hazardous Methylene Blue from Aqueous Solution using Combustion Derived $\text{CaAl}_2\text{O}_4$ Nanoparticles

B.M. Pradeep Kumar<sup>a</sup>, K.H. Shivaprasad<sup>a</sup>, R.S. Raveendra<sup>b</sup>, R. Hari Krishna<sup>c</sup>, B.M. Nagabhushana<sup>c\*</sup>

<sup>a</sup>Department of Chemistry, VSK University, Bellary-583 104, India.

<sup>b</sup>Department of Chemistry, Sai Vidya Institute of Technology, Bengaluru-560 064, India.

<sup>c</sup>Department of Chemistry, M.S. Ramaiah Institute of Technology, Bengaluru -560 054, India.

### Article history

Received: 02-Nov-2016

Revised: 20-Nov-2016

Available online: 02-Dec-2016

### Keywords:

Adsorption,  
Combustion,  
Synthesis,  
PXRD

### Abstract

In this article  $\text{CaAl}_2\text{O}_4$  nanoparticles were prepared using a facile self-propagating solution combustion synthesis (SCS) using oxalyldihydrazide (ODH) as fuel. PXRD results shows that all the diffraction peaks are well matched with ICDD card number 53-191 and found to be monoclinic structure. FTIR spectrum reveals the vibrational frequency of metal – oxygen bond and purity of the nanoparticles. Optical energy band gap was calculated from the Wood-Tauc relation using UV-Vis spectrum which was found to be 5.0 eV. SEM micrograph shows porous and foamy morphology. Adsorption experiments were performed with cationic methylene blue (MB) dye and found 77 % dye was at 12 pH at contact time of 25 min of the contact time. The optimum adsorbent dose was found to be 0.8 g/L of dye.

© 2016 JMSSE All rights reserved

### Introduction

Currently synthetic dyes are extensively used in different fields, such as textile, paper, leather etc., and their direct discharge into waters causes various environmental troubles, which resulted from their carcinogenicity, toxicity to aquatic life and undesirable aesthetic aspect [1–5]. Majority of the dyes are toxic, mutagenic and carcinogenic in nature besides they are very stable to light, temperature and microbial attack, making them intractable compounds. From an environmental point of view, the removal of synthetic dyes is of great concern [6]. To decontaminate the dye pollutants, various technologies have been developed and applied, such as adsorption, electrolysis, advanced oxidation and active sludge method. Among all these commonly adopted methods, adsorption is regarded as the fast, efficient and general technology. Many categories of adsorbent materials are evaluated in dye removal [7-10]. Recently greater attention has been committed to the study of removal of dyes and pigments from industrial effluents and waste water by adsorption process using nano structured materials [11, 12]. Nanoparticles exhibit atom-like behaviour due to a high surface, a large fraction of surface atoms and the wide gap between valence and conduction band when divided to near atomic size [13].

As one of the common dyes, methylene blue (MB) is widely used as the colouring agent and disinfectant in rubbers, pharmaceuticals, pesticides and dyestuffs and so on. It has been reported that cationic dyes like MB are more toxic than anionic dyes; exposure of MB to human being will cause skin and eye irritation, carcinogenicity, reproductive and developmental toxicity, neurotoxicity and chronic toxicity. In this regard, an increased interest has been focused on the adsorptive removal of MB from the waste water [14-17]. Calcium aluminates are important cement materials, which have been studied by many researchers. Calcium aluminates ( $\text{CaO-Al}_2\text{O}_3$ ) are attractive ceramic materials for high temperature refractory applications. In

recent years, calcium aluminates based materials have found new applications in the field of advanced ceramics as optical ceramics, catalyst support, flame detectors, dental cements and structural ceramics [18, 19].

Objective of this study is to synthesize  $\text{CaAl}_2\text{O}_4$  nanoparticles by solution combustion synthesis and to study its effectiveness of adsorption of methylene blue dye.

### Experimental

#### Materials

Commercially pure calcium nitrate ( $\text{Ca}(\text{NO}_3)_2 \cdot 4\text{H}_2\text{O}$ , AR 99% Merck), aluminium nitrate ( $\text{Al}(\text{NO}_3)_3 \cdot 9\text{H}_2\text{O}$ , AR 99.99% Merck), ODH ( $\text{C}_2\text{H}_6\text{N}_4\text{O}_2$ ), hydrochloric acid (HCl Fisher scientific), hydroxide (NaOH Fisher scientific), MB dye ( $\text{C}_{16}\text{H}_{18}\text{ClN}_3\text{S}$ , Sigma-Aldrich), were used as such without further purification.

#### Synthesis of $\text{CaAl}_2\text{O}_4$ nanoparticles

$\text{CaAl}_2\text{O}_4$  nanoparticles were synthesized by solution combustion method [20-22]. The starting materials, calcium nitrate ( $\text{Ca}(\text{NO}_3)_2 \cdot 4\text{H}_2\text{O}$ ), aluminium nitrate ( $\text{Al}(\text{NO}_3)_3 \cdot 9\text{H}_2\text{O}$ ) are the sources of Ca, Al respectively and ODH was used as fuel. The stoichiometric amount of corresponding nitrates were taken in a crystalline dish and dissolved in distilled water and stirred the mixture for 30 minutes. The crystalline dish containing the heterogeneous redox mixture is introduced into a muffle furnace maintained at  $500 \pm 10$  °C. First the solution boils and undergoes dehydration. Eventually the mixture undergoes decomposition, which results in the liberation of large amounts of gases (usually  $\text{CO}_2$ ,  $\text{H}_2\text{O}$  and  $\text{N}_2$ ). This is followed by a spontaneous ignition which results in flame type combustion. The whole process is over in less than 5 min and a highly  $\text{CaAl}_2\text{O}_4$  nanopowder is obtained as per the following chemical equation



### Preparation of Methylene blue dye solution

An accurately weighed amount (10 mg) of the MB dye was dissolved in 1000 ml distilled water to prepare 10 ppm stock solution.

### Characterization techniques

The product was characterized by PXRD. Powder X-ray diffraction patterns were collected on a Shimadzu XRD-700 X-ray Diffractometer with CuK $\alpha$  radiation with diffraction angle range  $2\theta = 20^\circ$  to  $80^\circ$ , operating at 40 kV and 30 mA. The FT-IR studies have been performed on a Perkin Elmer Spectrometer (Spectrum 1000) with KBr pellet technique in the range of 400-4000  $\text{cm}^{-1}$ . To calculate optical energy band gap, UV-Vis spectrum was recorded using specord 800 UV-Vis spectrophotometer. Product was morphologically characterized by SEM performed on a ZEISS scanning electron microscope with a voltage of 5 kV.

## Results and Discussion

Figure 1 represents the PXRD pattern of the product obtained by SCS. The product is crystalline and show well resolved peaks corresponding to all the planes of standard monoclinic CaAl<sub>2</sub>O<sub>4</sub> (ICDD: 53-191). All the diffraction peaks can be indexed to (1 1 2), (2 2 0), (3 0 1), (0 0 6) (3 0 3), (0 3 2), (0 4 0), (4 7 2) and (3 4 3) reflections. The crystallite size is calculated from the full width at half maximum (FWHM ( $\beta$ )) of the diffraction peaks using Debye- Scherer's method [23] using the following equation,

$$d = \frac{k\lambda}{\beta \cos \theta} \quad (2)$$

Where 'd' is the average crystalline dimension perpendicular to the reflecting phases, ' $\lambda$ ' is the X-ray wavelength, 'k' is shape factor, ' $\beta$ ' is the full width at half maximum (FWHM) intensity of a Bragg reflection excluding instrumental broadening and ' $\theta$ ' is the Bragg's angle. The calculated average crystallite size of the product is found in the range of 40-45 nm.

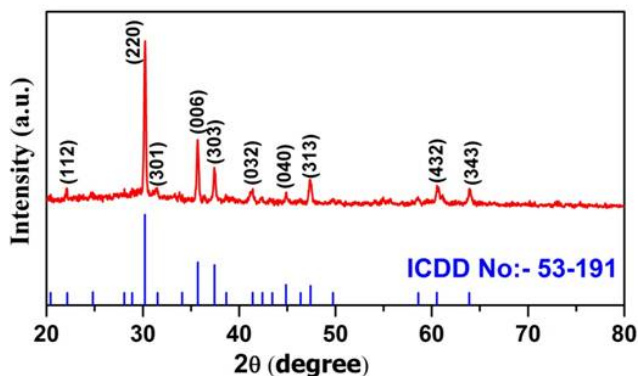


Figure 1: PXRD of CaAl<sub>2</sub>O<sub>4</sub> nanoparticles

Figure 2 represents FT-IR spectrum of the sample recorded to define the vibrational frequency of metal – oxygen in the CaAl<sub>2</sub>O<sub>4</sub> nanoparticles. It can be seen that no major impurity peaks corresponding to the organic impurities was observed. However, a weak band can be seen at 2365  $\text{cm}^{-1}$  which is ascribed to the stretching vibration of the C–H band in ODH. Another small peak at 1470  $\text{cm}^{-1}$  is due to the nitro group of the precursors. A broad peak at 3501  $\text{cm}^{-1}$  is attributed to OH band of water molecules. Strong absorption bands at 813  $\text{cm}^{-1}$  and 643  $\text{cm}^{-1}$  can be assigned to the stretching vibration of M–O bonds (M= Ca, Al) [24].

In order to determine the optical energy band gap of sample, the UV-Vis absorption spectrum was recorded. Fig. 3 (a) shows the

UV-Vis absorption spectrum of sample. The sample shows a strong absorption peak ( $\lambda_{\text{max}}$ ) at 205 nm at the UV region. This can be attributed to photo excitation of electron from valence band to conduction band. The optical energy band gap ( $E_g$ ) was estimated (Fig. 3 (b)) by the method proposed by Wood and Tauc [25] according to the following equation,

$$(h\nu\alpha)^n (h\nu - E_g) \quad (3)$$

where ' $\alpha$ ' is the absorbance, ' $h$ ' is the Planck constant, ' $\nu$ ' is the frequency, ' $E_g$ ' is the optical energy band gap and ' $n$ ' is a constant associated to the different types of electronic transitions ( $n= 1/2, 2, 3/2$  or 3 for direct allowed, indirect allowed, direct forbidden and indirect forbidden transitions, respectively).  $E_g$  value for CaAl<sub>2</sub>O<sub>4</sub> nanoparticles is  $\sim 5.0$  eV which is well agreement with the literature.

The scanning electron micrograph of CaAl<sub>2</sub>O<sub>4</sub> nanoparticles is shown in Fig.4. The powder shows foamy disconnected structures with significant porous and loosely packed particle clusters. The agglomeration of particles in sample might be due to high exothermic nature of the reaction resulting in partial sintering of the particles.

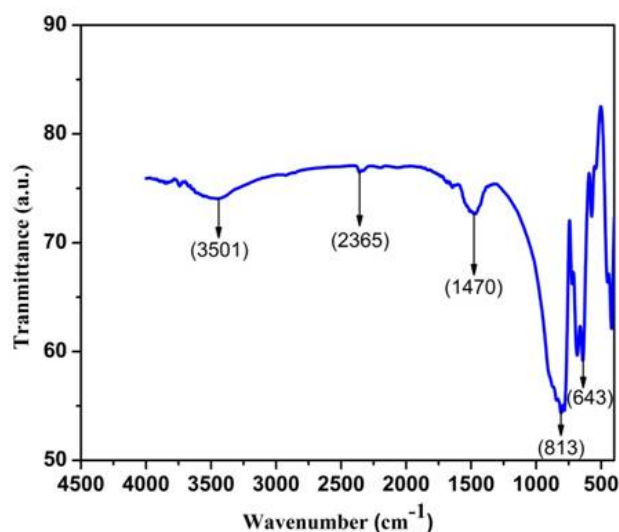


Figure 2: FTIR spectrum of CaAl<sub>2</sub>O<sub>4</sub> nanoparticles

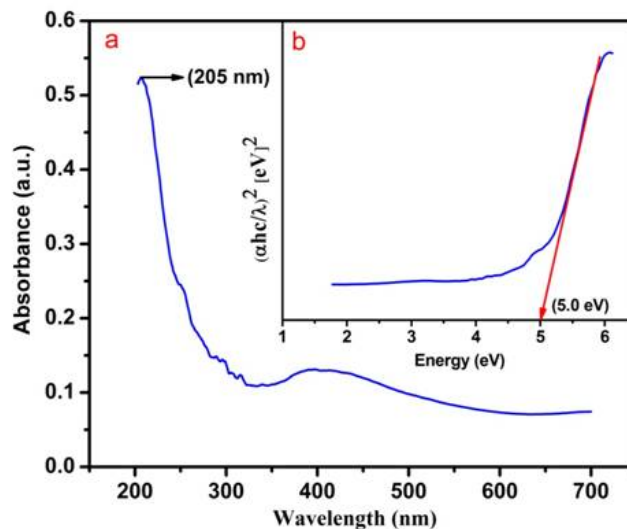


Figure 3: (a) UV-Vis spectrum (b) Optical energy band gap of CaAl<sub>2</sub>O<sub>4</sub> nanoparticles

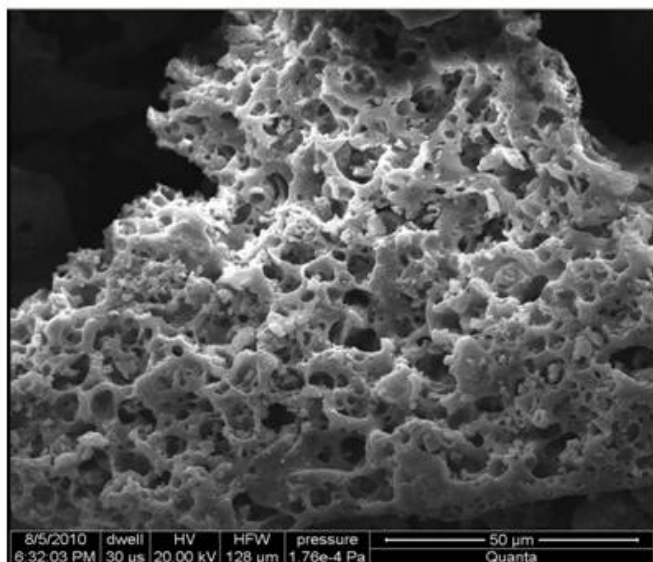


Figure 4: SEM micrograph of CaAl<sub>2</sub>O<sub>4</sub> nanoparticles

Adsorption studies

Adsorption experiments were performed using organic hazardous cationic MB dye. MB is a heterocyclic aromatic chemical compound with a chemical formula C<sub>16</sub>H<sub>18</sub>ClN<sub>3</sub>S. IUPAC name of MB is 3, 7 bis (Dimethylamino)-phenothiazin-5-ium chloride. Molecular structure of MB is as follows.

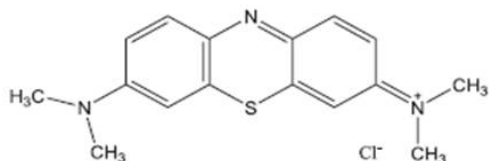


Figure 5: Molecular structure of Methylene blue dye

Batch experiments were carried out at different time, dose and pH. 50 ml of dye solution of 10 ppm was mixed with different dose of adsorbent in 250 ml conical flask at room temperature. The dye solution is separated from the adsorbent by centrifugation at 1800 rpm for 5 min. Residual concentration of dye in supernatant was estimated spectrophotometrically by monitoring the absorbance at 665 nm ( $\lambda_{max}$ ) using a UV-Vis spectrophotometer.

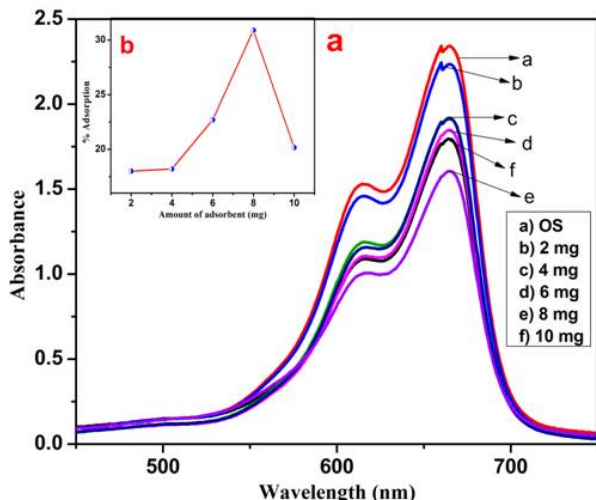


Figure 6: (a) Effect of dosage, (b) Percentage adsorption plot

Effect of dosage

Adsorption of dye is strongly influenced by the amount of the adsorbent. Adsorption of MB onto CaAl<sub>2</sub>O<sub>4</sub> nanoparticles was studied with changing the amount of adsorbent from 2 mg to 10 mg at a constant stirring rate of 30 minutes with concentration of 10 ppm of 50 ml dye solution. It is observed from the Fig. 6(a-b) that with increase in the dose, adsorption of MB increases upto optimum quantity of adsorbent. Maximum of 31% dye adsorbed at the dose of 8 mg of adsorbent. Further increase in adsorbent dose, decreases the adsorption percentage. This might be attributed to over-lapping or aggregation of adsorption sites resulting in decrease in total adsorbent surface area available to MB and increase in path length [26].

Effect of contact time

Effect of contact time on the adsorption of MB onto CaAl<sub>2</sub>O<sub>4</sub> nanoparticles was studied by optimized quantity of adsorbent and at room temperature. It can be observed from the Fig. 7 (a-b) that the dye adsorption increases with the increasing of stirring time. The rate of adsorption is initially quite rapid with most of the compound being adsorbed within the first 25 min. It was found that more than 35% adsorption of dye occurred in the first 25 min; thereafter the rate of adsorption was found to be slow. This shows that equilibrium can be assumed to be achieved after 25 min. It is basically due to saturation of the active site which does not allow further adsorption to take place [27].

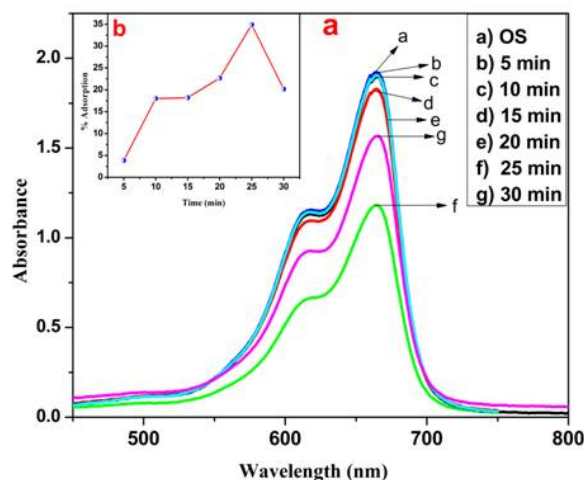


Figure 7: (a) Effect of stirring, (b) Percentage adsorption plot

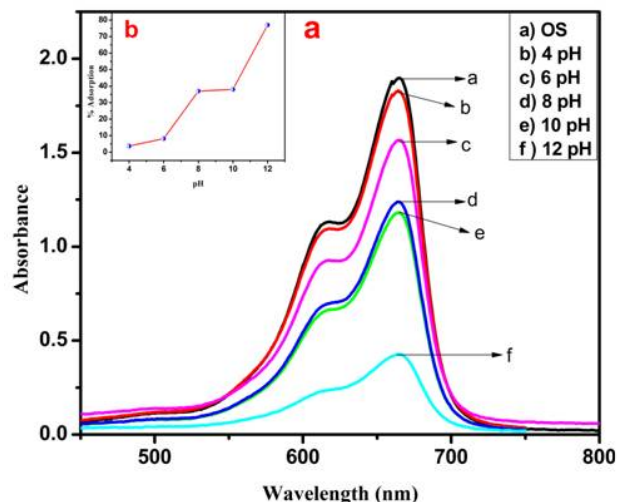


Figure 8: (a) Effect of pH, (b) Percentage adsorption plot

### Effect of pH

The pH of system has a great effect on the adsorption efficiency of organic dyes. Effect of pH on MB adsorption onto the CaAl<sub>2</sub>O<sub>4</sub> nanoparticles was carried out at 10 ppm of initial dye concentration with 8 mg mass of adsorbent at 25 min of stirring rate at room temperature. As given in the Fig. 8(a-b), CaAl<sub>2</sub>O<sub>4</sub> nanoparticles show maximum of 77% dye adsorption at the pH of 12 which decreased to 4% at pH of 4. This confirms that the high pH (10-12) is favourable for MB adsorption. This is due to the fact that MB is a cationic dye. Its adsorption increases when the surface of the adsorbent is negatively charged.

### Mechanism of adsorption of MB onto CaAl<sub>2</sub>O<sub>4</sub> nanoparticles

Mechanism of adsorption of MB onto the CaAl<sub>2</sub>O<sub>4</sub> nanoparticles can be explained on the basis of pH effect [28]. Under acidic conditions, it is difficult for cationic MB dye to adsorb onto the CaAl<sub>2</sub>O<sub>4</sub> surface. This is because, as initial pH of dye solution decreased, the number of negatively charged adsorbent sites decreased and positively charged sites increased which did not favour the adsorption since the MB is a cationic dye results in electrostatic repulsion. This decrease in the adsorption at lower pH is also due to the fact that the presence of excess H<sup>+</sup> released from the MB dye at acidic condition which opposing with dye cations for the adsorption. In turn at higher pH the negatively charged sites on adsorbent molecule increases which attracts the positively charged sites of cationic MB dye results in high adsorption.

### Conclusions

The single phase of CaAl<sub>2</sub>O<sub>4</sub> nanoparticles were successfully prepared by the simple SCS method and its adsorption capacity for MB dye was investigated. The result showed that the parameters like effect of pH and contact time will play a very important role on the adsorption.

### Acknowledgments

The author B.M. Pradeep Kumar thanks the department of chemistry, VSK University, Bellary for the support to publish this article and the author R.S. Raveendra thank the Principal and management of Sai Vidya Institute of Technology for their constant encouragement.

### References

1. E. El-Qada, S.J. Allen, G.M. Walker, Adsorption of basic dyes from aqueous solution onto activated carbons, *Chem. Eng. J.* 135 (2008) 174–184.
2. V.K. Gupta, Suhas, Application of low-cost adsorbents for dye removal—a review, *J. Environ. Manage.* 90 (2009) 2313–2342.
3. C.A.P. Almeida, N.A. Debacher, A.J. Downs, L. Cottet, C.A.D. Mello, Removal of methylene blue from colored effluents by adsorption on montmorillonite clay, *J. Colloid Interface Sci.* 332 (2009) 46–53.
4. I. Kunczek, S. Sener, Adsorption of methylene blue onto sonicated sepiolite from aqueous solutions, *Ultrason. Sonochem.* 17 (2010) 250–257.
5. V. Ponnusami, K.S. Rajan, S.N. Srivastava, Application of film-pore diffusion model for methylene blue adsorption onto plant leaf powders, *Chem. Eng. J.* 163 (2010) 236–242.
6. Raveendra R.S., Prashanth P.A., Malini B.R., Nagabhushana B.M., Adsorption of Eriochrome black-T azo Dye from Aqueous solution on Low cost Activated Carbon prepared from Tridax procumbens, *Research Journal of Chemical Science.* 5(3) (2015) 9–13.
7. Y. Zhang, I. Angelidaki, Microbial electrolysis cells turning to be versatile technology: recent advances and future challenges, *Water Res.* 56 (2014) 11–25.
8. I. Sires, E. Brillas, Remediation of water pollution caused by pharmaceutical residues based on electrochemical separation and degradation technologies: a review, *Environ. Int.* 40 (2012) 212–229.
9. M. Rafatullah, O. Sulaiman, R. Hashim, A. Ahmad, Adsorption of methylene blue on low-cost adsorbents: a review, *J. Hazard. Mater.* 177 (2010) 70–80.
10. D. Mohan, C. Pittman, Activated carbons and low cost adsorbents for remediation of tri- and hexavalent chromium from water, *J. Hazard. Mater.* 137 (2006) 762–811.
11. R.S. Raveendra, P.A. Prashanth, R. Hari Krishna, N.P. Bhagya, B.M. Nagabhushana, H. Raja Naika, K. Lingaraju, H. Nagabhushana and B. Daruka Prasad, Solution combustion derived nanocrystalline ZnTiO<sub>3</sub>: Effective adsorbent and antibacterial agent, *J.Asian Ceram. Soc.*, 2, (2014) 357–365.
12. Wang, J.-Q., Liu, Y.-H., Chen, M.-W., Louzguine-Luzgin, D. V, Inoue, A., & Perepezko, J. H. Excellent capability in degrading azo dyes by Mg-Zn-based metallic glass powders. *Scientific reports*, 2, (2012) 418.
13. A.V. Dijken, E.A. Meulenkaamp, D.Vanmaekelbergh, A. Meijerink, Identification of the transition responsible for the visible emission in ZnO using quantum size effect, *J. Lumin.* 90 (2000) 123–128.
14. F. Zhang, Z. Zhao, R. Tan, Y. Guo, L. Cao, L. Chen, J. Li, W. Xu, Y. Yang, W. Song, Selective and effective adsorption of methyl blue by barium phosphate nano-flake, *J. Colloid Interface Sci.* 386 (2012) 277–284.
15. Hao, O.J., Kim, H and Chiang, P.C, Decolonization of wastewater. *Critical Reviews in Environmental Science and Technology*, 30 (2000) 449–505.
16. N. Gupta, A.K. Kushwaha, M.C. Chattopadhyaya, Adsorption studies of cationic dyes onto Ashoka (saraca asoca) leaf powder, *J. Taiwan Inst. Chem. Eng.* 43 (2012) 604–613.
17. M. A. Brown and S. C. De Vito, “Predicting azo dye toxicity,” *Critical Reviews in Environmental Science and Technology*, 23(3) (1993) 249–324.
18. B. M. Mohamed, J. H Sharp, Kinetics and mechanism of formation of monocalcium Aluminate- CaAl<sub>2</sub>O<sub>4</sub>. *J. Mater. Chem.* 7 (1997) 595–1599.
19. M. M. Ali., S. K. Agarwal., S. K. Handoo, Diffusion studies in formation and sintering of CaAl<sub>2</sub>O<sub>4</sub> and BaAl<sub>2</sub>O<sub>4</sub>. *Cement and Concrete Research.* 27 (1997) 979–982.
20. K. C. Patil, S. T. Aruna, T. Mimani, Combustion synthesis: an update, *Curr. Opin. Solid State Mater. Sci.* 6(6) (2002) 507–512.
21. P. A. Prashanth, R. S. Raveendra, R. H. Krishna, N. P. Bhagya, S. Ananda, B. M. Nagabhushana, K. Lingaraju, H. R. Naika, Synthesis, characterizations, antibacterial and photoluminescence studies of solution combustion-derived α-Al<sub>2</sub>O<sub>3</sub> nanoceramic, *J. Asian Ceram. Soc.* 3 (2015) 345–351.
22. R. S. Raveendra, P. A. Prashanth, B. M. Nagabhushana, Study on the effect of fuels on phase formation and morphology of combustion derived α-Al<sub>2</sub>O<sub>3</sub> and NiO nanomaterials, *Adv. Mater. Lett.* 7 (2016) 216–220.
23. H.P. Klug, LE Alexander, X-ray Diffraction Procedure, Wiley, New York, (1954).
24. Y.L. Chai, Y.S. Chang, G. J. Chen, Y. Hsiao, The effects of heat-treatment on the structure evolution and crystallinity of ZnTiO<sub>3</sub> nanocrystals prepared by Pechini process, *J. Mater. Res. Bull.* 43(5) (2008) 1066–1073.
25. J. Tauc and F. Abeles (Ed.), *Optical Properties of Solids*, North-Holland, Amsterdam. (1970).
26. V. K. Garg, Moirangthem Amita, Rakesh Kumar, and Renuka Gupta, Basic dye (methylene blue) removal from simulated wastewater by adsorption using Indian Rosewood sawdust: a timber industry waste, *Dyes. Pigments.* 63 (2004) 243–250.
27. Mi-Hwa Baek, Christianah Olakitan Ijagbemi, and Dong-Su Kim, Removal of Malachite Green from aqueous solution using degreased coffee bean *J. Hazard. Mater.*, 176 (2010) 820–828.
28. Emine Akar, Aylin Altinisik, and Yoldas Seki, Using of activated carbon produced from spent tea leaves for the removal of malachite green from aqueous solution, *Ecol. Engin.*, 52 (2013) 19–27.

